INTERPRETATIONS ARE USEFUL: PENALIZING EXPLANATIONS TO ALIGN NEURAL NETWORKS WITH PRIOR KNOWLEDGE

Anonymous authors
Paper under double-blind review

ABSTRACT

For an explanation of a deep learning model to be effective, it must provide both insight into a model and suggest a corresponding action in order to achieve some objective. Too often, the litany of proposed explainable deep learning methods stop at the first step, providing practitioners with insight into a model, but no way to act on it. In this paper, we propose contextual decomposition explanation penalization (CDEP), a method which enables practitioners to leverage existing explanation methods in order to increase the predictive accuracy of deep learning models. In particular, when shown that a model has incorrectly assigned importance to some features, CDEP enables practitioners to correct these errors by directly regularizing the provided explanations. Using explanations provided by contextual decomposition (CD) (Murdoch et al., 2018), we demonstrate the ability of our method to increase performance on an array of toy and real datasets.

1 INTRODUCTION

In recent years, neural networks have demonstrated strong predictive performance across a wide variety of settings. However, in order to achieve that accuracy, they sometimes latch onto spurious correlations, leading to undesirable behavior as a result of dataset bias (Winkler et al., 2019), racial and ethnic stereotypes (Garg et al., 2018), or simply overfitting. While recent work into explaining neural network predictions (Murdoch et al., 2019; Doshi-Velez & Kim, 2017) has demonstrated an ability to uncover the relationships learned by a model, it is still unclear how to actually alter the model in order to remove incorrect, or undesirable, relationships.

We introduce contextual decomposition explanation penalization (CDEP), a method which leverages existing explanation techniques for neural networks in order to prevent a model from learning unwanted relationships and ultimately improve predictive accuracy. Given particular importance scores, CDEP works by allowing the user to directly penalize importances of certain features, or interactions. This forces the neural network to not only produce the correct prediction, but also the correct explanation for that prediction. While we focus on contextual decomposition (CD) (Murdoch et al., 2018; Singh et al., 2018), which allows the penalization of both feature importances and interactions, CDEP can be readily adapted for existing interpretation techniques, as long as they are differentiable. Moreover, CDEP is a general technique, which can be applied to arbitrary neural network architectures, and is orders of magnitude faster and more memory efficient than recent gradient-based methods, allowing its use on meaningful datasets.

In order to demonstrate the effectiveness of CDEP, we conducted experiments across a wide variety of tasks. In the prediction of skin cancer from images, CDEP improves the prediction of a classifier by teaching it to ignore spurious confounding variables present in the training data. In a colored MNIST task, CDEP allows the network to focus on a digit's shape rather than its color (with no extra human annotation needed). Finally, a toy example using text classification shows how the penalization can help a network avoid a bias towards particular words, such as those involving gender.

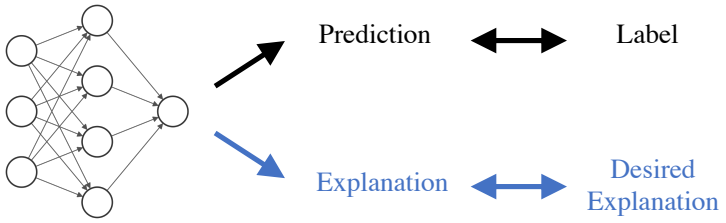

Figure 1: CDEP allows a practitioner to penalize both a model's prediction and the corresponding explanation

2 BACKGROUND

Explanation methods Many methods have been developed to help explain the learned relationships contained in a DNN. For local, or prediction-level, explanation, most prior work has focused on assigning importance to individual features, such as pixels in an image or words in a document. There are several methods that give feature-level importance for different architectures. They can be categorized as gradient-based (Springenberg et al., 2014; Sundararajan et al., 2017; Selvaraju et al., 2016; Baehrens et al., 2010; Rieger & Hansen, 2019), decomposition-based (Murdoch & Szlam, 2017; Shrikumar et al., 2016; Bach et al., 2015) and others (Dabkowski & Gal, 2017; Fong & Vedaldi, 2017; Ribeiro et al., 2016; Zintgraf et al., 2017), with many similarities among the methods (Ancona et al., 2018; Lundberg & Lee, 2017). However, many of these methods have thus far been poorly evaluated (Adebayo et al., 2018; Nie et al., 2018), casting doubt on their usefulness. Another line of work, which we build upon, has focused on uncovering interactions between features, in addition to feature importances, (Murdoch et al., 2018), and using those interactions to create a hierarchy of features displaying the model's prediction process (Singh et al., 2018).

Uses of explanation methods While much work has been put into developing methods for explaining DNNs, relatively little work has explored the potential to use these explanations to help build a better model. Some recent work proposes forcing models to attend to regions of the input which are known to be important (Burns et al., 2018; Mitsuhara et al., 2019), although it is important to note that attention is often not the same as explanation (Jain & Wallace, 2019). An alternative line of work proposes penalizing the gradients of a neural network to match human-provided binary annotations and shows the possibility to improve performance (Ross et al., 2017) and adversarial robustness (Ross & Doshi-Velez, 2018). Finally, two recent papers extend these ideas by penalizing attributions for natural language models (Liu & Avci, 2019) and penalizing a modified gradient-based score to produce smooth attributions (Erion et al., 2019).

Other ways to constrain DNNs While we focus on the use of explanations to constrain the relationships learned by neural networks, other approaches for constraining neural networks have also been proposed. A computationally intensive alternative is to augment the dataset in order to prevent the model from learning undesirable relationships, through domain knowledge (Bolukbasi et al., 2016), projecting out superficial statistics (Wang et al., 2019) or dramatically altering training images (Geirhos et al., 2018). However, these processes are often not feasible, either due to their computational cost or the difficulty of constructing such an augmented data set. Adversarial training has also been explored (Zhang & Zhu, 2019). These techniques are generally limited, as they are often tied to particular datasets, and do not provide a clear link between learning about a model's learned relationships through explanations, and subsequently correcting them.

3 METHODS

We now introduce CDEP, which penalizes the explanations of a neural network in order to align with prior knowledge about why a model should make a prediction. To do so, for each data point it penalizes the CD scores of features, or groups of features, which a user does not want the model to learn to be important. While we focus on CD scores, which allow the penalization of interac-

tions between features in addition to features themselves, this approach readily generalizes to other interpretation techniques, so long as they are differentiable.

3.1 AUGMENTING THE LOSS FUNCTION

Given a particular classification task, we want to teach a model to not only produce the correct prediction, but also to arrive at the prediction for the correct reasons. That is, we want the model to be right for the right reasons, where the right reasons are provided by the user and are dataset-dependent.

To accomplish this, CDEP modifies the objective function used to train a neural network, as displayed in Eq 1. In addition to the standard prediction loss $\mathcal{L}$, which teaches the model to produce the correct predictions, CDEP adds an explanation error $\mathcal{L}_{\text{expl}}$, which teaches the model to produce the correct explanations for its predictions. In place of the prediction and labels $f_\theta(X), y$, used in the prediction error $\mathcal{L}$, the explanation error $\mathcal{L}_{\text{expl}}$ uses the explanations produced by an interpretation method $\text{expl}_\theta(X)$, along with targets provided by the user expl_X. As is common with penalization, the two losses are weighted by a hyperparameter $\lambda \in \mathbb{R}$:

$$\hat{\theta} = \underset{\theta}{\text{argmin}} \underbrace{\mathcal{L}\left(f_\theta(X), y\right)}_{\text{Prediction error}} + \lambda \underbrace{\mathcal{L}_{\text{expl}}\left(\text{expl}_\theta(X), \text{expl}_X\right)}_{\text{Explanation error}} \tag{1}$$

The precise meanings of expl_X depend on the context. For example, in the skin cancer image classification task described in Section 4, many of the benign skin images contain band-aids, but none of the malignant images. To force the model to ignore the band-aids in making their prediction, in each image $\text{expl}_\theta(X)$ denotes the importance score of the band-aid and expl_X would be zero. These and more examples are further explored in Section 4.

3.2 CONTEXTUAL DECOMPOSITION (CD)

In this work, we use the CD score as the explanation function. In contrast to other interpretation methods, which focus on feature importances, CD also captures interactions between features. CD was originally designed for LSTMs (Murdoch et al., 2018) and subsequently extended to convolutional neural networks and arbitrary DNNs (Singh et al., 2018). For a given DNN $f(x)$, one can represent its output as a SoftMax operation applied to logits $g(x)$. These logits, in turn, are the composition of L layers g_i, such as convolutional operations or ReLU non-linearities.

$$f(x) = \text{SoftMax}(g(x)) = \text{SoftMax}(g_L(g_{L-1}(...(g_2(g_1(x)))))) \tag{2}$$

Given a group of features $\{x_j\}_{j \in S}$, the CD algorithm, $g^{CD}(x)$, decomposes the logits $g(x)$ into a sum of two terms, $\beta(x)$ and $\gamma(x)$. $\beta(x)$ is the importance score of the feature group $\{x_j\}_{j \in S}$, and $\gamma(x)$ captures contributions to $g(x)$ not included in $\beta(x)$. The decomposition is computed by iteratively applying decompositions $g_i^{CD}(x)$ for each of the layers $g_i(x)$.

$$g^{CD}(x) = g_L^{CD}(g_{L-1}^{CD}(...(g_2^{CD}(g_1^{CD}(x))))) = (\beta(x), \gamma(x)) \tag{3}$$

$$\beta(x) + \gamma(x) = g(x) \tag{4}$$

3.3 CDEP OBJECTIVE FUNCTION

We now substitute the above CD scores into the generic equation in Eq 1 to arrive at the method used in this paper. While we use CD for the explanation method $\text{expl}_\theta(X)$, other explanation methods could be readily substituted at this stage. In order to convert CD scores to probabilities, we apply a SoftMax operation to $g^{CD}(x)$, allowing for easier comparison with the user-provided labels expl_X. We collect from the user, for each input x_i, a collection of feature groups $x_{i,S}$, $x_i \in \mathbb{R}^d, S \subseteq \{1, ..., d\}$, along with explanation target values $\text{expl}_{x_{i,S}}$, and use the $\| \cdot \|_1$ loss for $\mathcal{L}_{\text{expl}}$.

$$\hat{\theta} = \underset{\theta}{\text{argmin}} \underbrace{\sum_i \sum_c -y_{i,c} \log f_\theta(x_i)_c}_{\text{Classification error}} + \lambda \underbrace{\sum_i \sum_S ||\beta(x_{i,S}) - \text{expl}_{x_{i,S}}||_1}_{\text{Explanation error}} \tag{5}$$

In the above, i indexes each individual example in the dataset, S indexes a subset of the features for which we penalize their explanations, and c sums over each class. Updating the model parameters in accordance with this formulation ensures that the model not only predicts the right output but also does so for the right (aligned with prior knowledge) reasons.

3.4 Computational considerations

A similar idea to Eq 1 has been proposed in previous/concurrent work, where the choice of explanation method uses a gradient-based attribution method (Ross et al., 2017; Erion et al., 2019). However, using such methods leads to three main complications which are solved by our approach. The first complication is the optimization process. When optimizing over attributions from a gradient-based attribution method via gradient descent, the optimizer requires the gradient of the gradient, thus requiring that all network components be twice differentiable. This process is computationally expensive and indeed optimizing it exactly involves optimizing over a differential equation. In contrast, CD attributions are calculated along with the forward pass of the network, and as a result can be optimized plainly with back-propagation using the standard single forward-pass and backward-pass per batch.

A second complication solved by the use of CD in Eq 5 is the ability to quickly finetune a pre-trained network. In many applications, particularly in transfer learning, it is common to finetune only the last few layers of a pre-trained neural network. Using CD, one can freeze early layers of the network and then finetune the last few layers of the network quickly as the activations and gradients of the frozen layers are not necessary.

Third, penalizing gradient-based methods incurs a very large memory usage. Using gradient-based methods, training requires the storage of activations and gradients for all layers of the network as well as the gradient of input (which can be omitted in normal training). Even for the simplest version, based on saliency, this more than doubles the required memory for a given batch and network size. More advanced methods proved to be completely infeasible to apply to a real-life dataset used, since the memory requirements were too high. By contrast, penalizing CD only requires a small constant amount of memory more than standard training.

4 Results

The results here demonstrate the efficacy of CDEP on a variety of datasets using diverse explanation types. Sec 4.1 shows results on ignoring spurious patches in the ISIC skin cancer dataset (Codella et al., 2019), Sec 4.2 details experiments on converting a DNN's preference for color to a preference for shape on a variant of the MNIST dataset (LeCun, 1998), and Sec 4.3 shows experiments on text data from the Stanford Sentiment Treebank (SST) (Socher et al., 2013).[1]

4.1 Ignoring spurious signals in skin cancer diagnosis

In recent years, deep learning has achieved impressive results in diagnosing skin cancer, with predictive accuracy sometimes comparable to human doctors (Esteva et al., 2017). However, the datasets used to train these models often include spurious features which make it possible to attain high test accuracy without learning the underlying phenomena (Winkler et al., 2019). In particular, a popular dataset from ISIC (International Skin Imaging Collaboration) has colorful patches present in approximately 50% of the non-cancerous images but not in the cancerous images (Codella et al., 2019). An unpenalized DNN learns to look for these patches as an indicator for predicting that an image is benign. We use CDEP to remedy this problem by penalizing the DNN placing importance on the patches during training.

The task in this section is to classify whether an image of a skin lesion contains (1) benign melanoma or (2) malignant melanoma. The ISIC dataset consists of 21,654 images (19,372 benign), each diagnosed by histopathology or a consensus of experts. For classification, we use a VGG16 architecture (Simonyan & Zisserman, 2014) pre-trained on the ImageNet Classification task [2] and freeze the

[1] All models were trained in PyTorch.

[2] Pre-trained model retrieved from torchvision.

weights of early layers so that only the fully connected layers are trained. In order to use CDEP, the spurious patches are identified via a s imple image segmentation algorithm using a color threshold (see Sec S1.4).

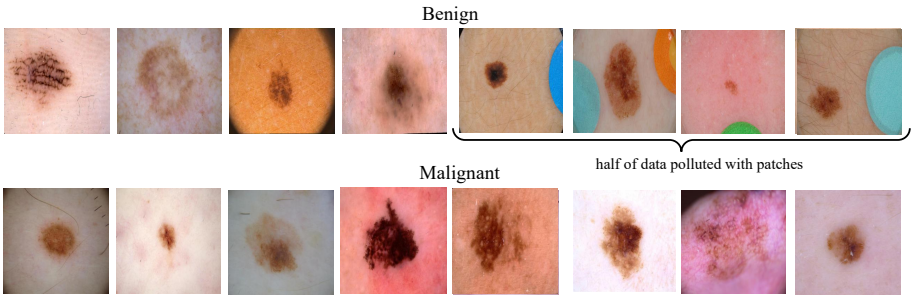

Figure 2: Example images from the ISIC dataset. Half of the benign lesion images include a patch in the image.

Table 1 shows results comparing the performance of a model trained with and without CDEP. We report results on two variants of the test set. The first, which we refer to as "no patches" only contains images of the test set that do not include patches. The second also includes images with those patches. Training with CDEP improves the AUC and F1-score for both test sets.

Table 1: Results from training a DNN on ISIC to recognize skin cancer (averaged over three runs). Results shown for the entire test set and for only the images the test set that do not include patches ("no patches"). The network trained with CDEP generalizes better, getting higher AUC and F1 on both. Std below 0.006 for all AUC and below 0.012 for all F1.

	AUC (no patches)	F1 (no patches)	AUC (all)	F1 (all)
Vanilla (excluded data)	0.86	0.59	0.92	0.59
Vanilla	0.85	0.56	0.92	0.56
With RRR	0.66	0.39	0.82	0.39
With CDEP	**0.88**	**0.61**	**0.93**	**0.61**

In the first row of Table 1, the model is trained using only the data without the spurious patches, and the second row shows the model trained on the full dataset. The network trained using CDEP achieves the best AUC, surpassing both unpenalized versions. Applying our method increases the ROC AUC as well as the best F1 score. We also compared our method against the method introduced in 2017 by Ross et al. (RRR). For this, we restricted the batch size to 16 (and consequently use a learning rate of 10^{-5}) due to memory constraints. Using RRR did not improve on the base AUC, implying that penalizing gradients is not helpful in penalizing higher-order features.[3]

Visualizing explanations Fig. 3 visualize GradCAM heatmaps (Ozbulak, 2019; Selvaraju et al., 2017) for an unpenalized DNN and a DNN trained with CDEP to ignore spurious patches. As expected, after penalizing with CDEP, the DNN attributes less importance to the spurious patches, regardless of their position in the image. More examples, also for cancerous images, are shown in Sec S1.5.

[3]We were not able to compare against the method recently proposed in Erion et al. (2019) due to the prohibitively slow training and large memory requirements.

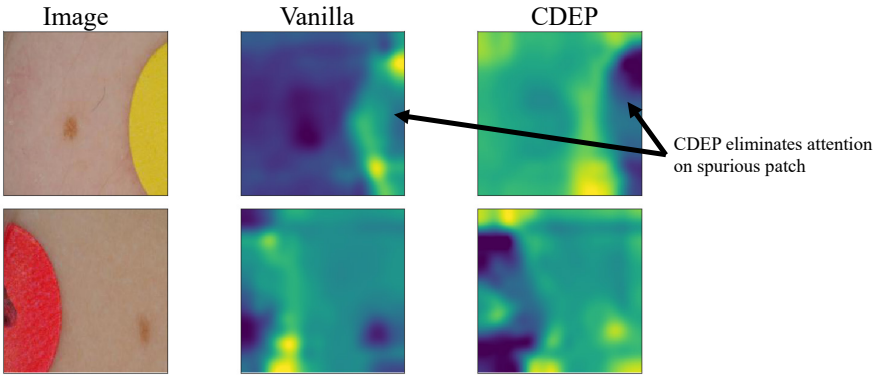

Figure 3: Visualizing heatmaps for correctly predicted exampes from the ISIC skincancer test set. Lighter regions in the heatmap are attributed more importance. The DNN trained with CDEP correctly captures that the patch is not relevant for classification.

4.2 Combating inductive bias on variants of the MNIST dataset

In this section, we investigate whether we can alter which features a DNN uses to perform digit classification, using variants of the MNIST dataset (LeCun, 1998) and a standard CNN architecture for this dataset retrieved from PyTorch [4].

4.2.1 ColorMNIST

Similar to a previous study (Li & Vasconcelos, 2019), we transform the MNIST dataset to include three color channels and assign each class a distinct color, as shown in Fig. 4. An unpenalized DNN trained on this biased data will completely misclassify a test set with inverted colors, dropping to 0% accuracy (see Section 4.2.1), suggesting that it learns to classify using the colors of the digits rather than their shape.

Here, we want to see if we can alter the DNN to focus on the shape of the digits rather than their color. Interestingly, this can be enforced by minimizing the contribution of pixels in isolation while maximizing the importance of groups of pixels (which can represent shapes). To do this, we add penalize the CD contribution of sampled single pixel values, following Eq 5. By minimizing the contribution of single pixels we effectively encourage the network to focus more on groups of pixels, which can represent shape.

Figure 4: ColorMNIST: the test set shapes remain the same as the training set, but the colors are inverted.

Section 4.2.1 shows that CDEP can partially change the network's focus on solely color to also focus on digit shape. We compare CDEP to two previously introduced explanation penalization techniques: penalization of the squared gradients (RRR) (Ross et al., 2017) and Expected Gradients (EG) (Erion et al., 2019). None of the baselines can improve the test accuracy of the model on this

[4]Model and training code from https://github.com/pytorch/examples/blob/master/mnist/main.py.

task above 0.6%, whereas CDEP is able to significantly improve this accuracy to 25.5%. We show the increase of predictive accuracy with increasing penalization in Fig. S5.

Table 2: Results on ColorMNIST (test accuracy). All values averaged over five runs. CDEP is the only method that captures and removes color bias.

	Unpenalized	CDEP	RRR	Expected Gradients
Test Accuracy	0.01 ± 0.2	25.5 ± 0.4	0.4 ± 0.2	0.4 ± 0.8

4.2.2 DECOYMNIST

For further comparison with previous work, we evaluate CDEP on an existing task: DecoyMNIST (Erion et al., 2019). DecoyMNIST adds a class-indicative gray patch to a random corner of the image. This task is relatively simple, as the spurious features are not entangled with any other feature and are always at the same location (the corners). Table 3 shows that all methods perform roughly equally, recovering the base accuracy.

Table 3 also shows that CDEP runs with relatively reasonable time and memory usage. It is similar to RRR, and considerable more feasible than Expected Gradients. However, when freezing early layers of a network, CDEP very quickly becomes more efficient than other methods. Results are reported using the best penalization parameter λ, chosen via cross-validation on the test accuracy. More details given in Sec S1.3.

Table 3: Results on Grayscale Decoy set.

	Unpenalized	CDEP	RRR	Expected Gradients
Test accuracy	60.1 ± 5.1	97.2 ± 0.8	99.0 ± 1.0	97.8 ± 0.2
Run time/epoch (seconds)	4.7	17.1	11.2	821.0
Maximum GPU RAM usage (GB)	0.027	0.068	0.046	3.15

4.3 FIXING BIAS IN TEXT DATA

To demonstrate CDEP's effectiveness on text, we use the Stanford Sentiment Treebank (SST) dataset (Socher et al., 2013), an NLP benchmark dataset consisting of movie reviews with a binary sentiment (positive/negative). We inject spurious signals into the training set and train a standard LSTM [5] to classify sentiment from the review.

[5] Model and training code from https://github.com/clairett/pytorch-sentiment-classification.

Positive

pacino is the best **she**'s been in years and keener is marvelous

she showcases davies as a young woman of great charm , generosity and diplomacy

shows **she** 's back in form , with an astoundingly rich film .

proves once again that **she**'s the best brush in the business

Negative

green ruins every single scene **he**'s in, and the film, while it 's not completely wreaked, is seriously compromised by that

i'm sorry to say that this should seal the deal - arnold is not, nor will **he** be, back .

this is sandler running on empty , repeating what **he** 's already done way too often .

so howard appears to have had free rein to be as pretentious as **he** wanted

Figure 5: Example sentences from the SST dataset with artificially induced bias on gender.

We create three variants of the SST dataset, each with different spurious signals which we aim to ignore (examples in Sec S1.1). In the first variant, we add indicator words for each class (positive: 'text', negative: 'video') at a random location in each sentence. An unpenalized DNN will focus only on those words, dropping to nearly random performance on the unbiased test set. In the second variant, we use two semantically similar words ('the', 'a') to indicate the class by using one word only in the positive and one only in the negative class. In the third case, we use 'he' and 'she' to indicate class (example in Fig 5). Since these gendered words are only present in a small proportion of the training dataset ($\sim 2\%$), for this variant, we report accuracy only on the sentences in the test set that do include the pronouns (performance on the test dataset not including the pronouns remains unchanged).

Table 4 shows the test accuracy for all datasets with and without CDEP. In all scenarios, CDEP is succesfully able to improve the test accuracy by ignoring the injected spurious signals.

Table 4: Results on SST. CDEP substantially improves predictive accuracy on the unbiased test set after training on biased data.

	Unpenalized	CDEP
Random words	56.6 ± 5.8	$\mathbf{75.4 \pm 0.9}$
Biased (articles)	57.8 ± 0.8	$\mathbf{68.2 \pm 0.8}$
Biased (gender)	64.2 ± 3.1	$\mathbf{78.0 \pm 3.0}$

5 Conclusion

In this work we introduce a novel method to penalize neural networks to align with prior knowledge. Compared to previous work, CDEP is the first of its kind that can penalize complex features and feature interactions. Furthermore, CDEP is more computationally efficient than previous work and does not rely on backpropagation, enabling its use with more complex neural networks. We show that CDEP can be used to remove bias and improve predictive accuracy on a variety of toy and real data. The experiments here demonstrate a variety of ways to use CDEP to improve models both on real and toy datasets. CDEP is quite versatile and can be used in many more areas to incorporate the structure of domain knowledge (e.g. biology or physics). Of course, the effectiveness of CDEP depends upon the quality of the prior knowledge used to determine the explanation targets. Future work includes extending CDEP to more complex penalties, incorporating more fine-grained explanations and interactions. We hope the work here will help push the field towards a more rigorous way to use interpretability methods, a point which will become increasingly important as interpretable machine learning develops as a field (Doshi-Velez & Kim, 2017; Murdoch et al., 2019).

REFERENCES

Radhakrishna Achanta, Appu Shaji, Kevin Smith, Aurelien Lucchi, Pascal Fua, and Sabine Süsstrunk. Slic superpixels compared to state-of-the-art superpixel methods. *IEEE transactions on pattern analysis and machine intelligence*, 34(11):2274–2282, 2012.

Julius Adebayo, Justin Gilmer, Michael Muelly, Ian Goodfellow, Moritz Hardt, and Been Kim. Sanity checks for saliency maps. In *Advances in Neural Information Processing Systems*, pp. 9505–9515, 2018.

Marco Ancona, Enea Ceolini, Cengiz Oztireli, and Markus Gross. Towards better understanding of gradient-based attribution methods for deep neural networks. In *6th International Conference on Learning Representations (ICLR 2018)*, 2018.

Sebastian Bach, Alexander Binder, Grégoire Montavon, Frederick Klauschen, Klaus-Robert Müller, and Wojciech Samek. On pixel-wise explanations for non-linear classifier decisions by layer-wise relevance propagation. *PloS one*, 10(7):e0130140, 2015.

David Baehrens, Timon Schroeter, Stefan Harmeling, Motoaki Kawanabe, Katja Hansen, and Klaus-Robert MÃžller. How to explain individual classification decisions. *Journal of Machine Learning Research*, 11(Jun):1803–1831, 2010.

Tolga Bolukbasi, Kai-Wei Chang, James Y Zou, Venkatesh Saligrama, and Adam T Kalai. Man is to computer programmer as woman is to homemaker? debiasing word embeddings. In *Advances in neural information processing systems*, pp. 4349–4357, 2016.

Kaylee Burns, Lisa Anne Hendricks, Kate Saenko, Trevor Darrell, and Anna Rohrbach. Women also snowboard: Overcoming bias in captioning models. *arXiv preprint arXiv:1803.09797*, 2018.

Noel Codella, Veronica Rotemberg, Philipp Tschandl, M Emre Celebi, Stephen Dusza, David Gutman, Brian Helba, Aadi Kalloo, Konstantinos Liopyris, Michael Marchetti, et al. Skin lesion analysis toward melanoma detection 2018: A challenge hosted by the international skin imaging collaboration (isic). *arXiv preprint arXiv:1902.03368*, 2019.

Piotr Dabkowski and Yarin Gal. Real time image saliency for black box classifiers. *arXiv preprint arXiv:1705.07857*, 2017.

Finale Doshi-Velez and Been Kim. Towards a rigorous science of interpretable machine learning. *arXiv preprint arXiv:1702.08608*, 2017.

Gabriel Erion, Joseph D Janizek, Pascal Sturmfels, Scott Lundberg, and Su-In Lee. Learning explainable models using attribution priors. *arXiv preprint arXiv:1906.10670*, 2019.

Andre Esteva, Brett Kuprel, Roberto A Novoa, Justin Ko, Susan M Swetter, Helen M Blau, and Sebastian Thrun. Dermatologist-level classification of skin cancer with deep neural networks. *Nature*, 542(7639):115, 2017.

Ruth C Fong and Andrea Vedaldi. Interpretable explanations of black boxes by meaningful perturbation. *arXiv preprint arXiv:1704.03296*, 2017.

Nikhil Garg, Londa Schiebinger, Dan Jurafsky, and James Zou. Word embeddings quantify 100 years of gender and ethnic stereotypes. *Proceedings of the National Academy of Sciences*, 115 (16):E3635–E3644, 2018. ISSN 0027-8424. doi: 10.1073/pnas.1720347115. URL `https://www.pnas.org/content/115/16/E3635`.

Robert Geirhos, Patricia Rubisch, Claudio Michaelis, Matthias Bethge, Felix A Wichmann, and Wieland Brendel. Imagenet-trained cnns are biased towards texture; increasing shape bias improves accuracy and robustness. *arXiv preprint arXiv:1811.12231*, 2018.

Sarthak Jain and Byron C Wallace. Attention is not explanation. *arXiv preprint arXiv:1902.10186*, 2019.

Yann LeCun. The mnist database of handwritten digits. *http://yann. lecun. com/exdb/mnist/*, 1998.

Yi Li and Nuno Vasconcelos. Repair: Removing representation bias by dataset resampling. *arXiv preprint arXiv:1904.07911*, 2019.

Frederick Liu and Besim Avci. Incorporating priors with feature attribution on text classification. *arXiv preprint arXiv:1906.08286*, 2019.

Scott M Lundberg and Su-In Lee. A unified approach to interpreting model predictions. In *Advances in Neural Information Processing Systems*, pp. 4768–4777, 2017.

Masahiro Mitsuhara, Hiroshi Fukui, Yusuke Sakashita, Takanori Ogata, Tsubasa Hirakawa, Takayoshi Yamashita, and Hironobu Fujiyoshi. Embedding human knowledge in deep neural network via attention map. *arXiv preprint arXiv:1905.03540*, 2019.

W James Murdoch and Arthur Szlam. Automatic rule extraction from long short term memory networks. *arXiv preprint arXiv:1702.02540*, 2017.

W James Murdoch, Peter J Liu, and Bin Yu. Beyond word importance: Contextual decomposition to extract interactions from lstms. *arXiv preprint arXiv:1801.05453*, 2018.

W James Murdoch, Chandan Singh, Karl Kumbier, Reza Abbasi-Asl, and Bin Yu. Interpretable machine learning: definitions, methods, and applications. *arXiv preprint arXiv:1901.04592*, 2019.

Weili Nie, Yang Zhang, and Ankit Patel. A theoretical explanation for perplexing behaviors of backpropagation-based visualizations. *arXiv preprint arXiv:1805.07039*, 2018.

Utku Ozbulak. Pytorch cnn visualizations. `https://github.com/utkuozbulak/pytorch-cnn-visualizations`, 2019.

Marco Tulio Ribeiro, Sameer Singh, and Carlos Guestrin. Why should i trust you?: Explaining the predictions of any classifier. In *Proceedings of the 22nd ACM SIGKDD International Conference on Knowledge Discovery and Data Mining*, pp. 1135–1144. ACM, 2016.

Laura Rieger and Lars Kai Hansen. Aggregating explainability methods for neural networks stabilizes explanations. *arXiv preprint arXiv:1903.00519*, 2019.

Andrew Slavin Ross and Finale Doshi-Velez. Improving the adversarial robustness and interpretability of deep neural networks by regularizing their input gradients. In *Thirty-second AAAI conference on artificial intelligence*, 2018.

Andrew Slavin Ross, Michael C Hughes, and Finale Doshi-Velez. Right for the right reasons: Training differentiable models by constraining their explanations. *arXiv preprint arXiv:1703.03717*, 2017.

Ramprasaath R Selvaraju, Michael Cogswell, Abhishek Das, Ramakrishna Vedantam, Devi Parikh, and Dhruv Batra. Grad-cam: Visual explanations from deep networks via gradient-based localization. *See https://arxiv. org/abs/1610.02391 v3*, 7(8), 2016.

Ramprasaath R Selvaraju, Michael Cogswell, Abhishek Das, Ramakrishna Vedantam, Devi Parikh, and Dhruv Batra. Grad-cam: Visual explanations from deep networks via gradient-based localization. In *Proceedings of the IEEE International Conference on Computer Vision*, pp. 618–626, 2017.

Avanti Shrikumar, Peyton Greenside, Anna Shcherbina, and Anshul Kundaje. Not just a black box: Learning important features through propagating activation differences. *arXiv preprint arXiv:1605.01713*, 2016.

Karen Simonyan and Andrew Zisserman. Very deep convolutional networks for large-scale image recognition. *arXiv preprint arXiv:1409.1556*, 2014.

Chandan Singh, W James Murdoch, and Bin Yu. Hierarchical interpretations for neural network predictions. *arXiv preprint arXiv:1806.05337*, 2018.

Richard Socher, Alex Perelygin, Jean Wu, Jason Chuang, Christopher D Manning, Andrew Ng, and Christopher Potts. Recursive deep models for semantic compositionality over a sentiment treebank. In *Proceedings of the 2013 conference on empirical methods in natural language processing*, pp. 1631–1642, 2013.

Jost Tobias Springenberg, Alexey Dosovitskiy, Thomas Brox, and Martin Riedmiller. Striving for simplicity: The all convolutional net. *arXiv preprint arXiv:1412.6806*, 2014.

Mukund Sundararajan, Ankur Taly, and Qiqi Yan. Axiomatic attribution for deep networks. *ICML*, 2017.

Haohan Wang, Zexue He, Zachary C Lipton, and Eric P Xing. Learning robust representations by projecting superficial statistics out. *arXiv preprint arXiv:1903.06256*, 2019.

Julia K. Winkler, Christine Fink, Ferdinand Toberer, Alexander Enk, Teresa Deinlein, Rainer Hofmann-Wellenhof, Luc Thomas, Aimilios Lallas, Andreas Blum, Wilhelm Stolz, and Holger A. Haenssle. Association Between Surgical Skin Markings in Dermoscopic Images and Diagnostic Performance of a Deep Learning Convolutional Neural Network for Melanoma RecognitionSurgical Skin Markings in Dermoscopic Images and Deep Learning Convolutional Neural Network Recognition of MelanomaSurgical Skin Markings in Dermoscopic Images and Deep Learning Convolutional Neural Network Recognition of Melanoma. *JAMA Dermatology*, 08 2019. ISSN 2168-6068. doi: 10.1001/jamadermatol.2019.1735. URL https://doi.org/10.1001/jamadermatol.2019.1735.

Tianyuan Zhang and Zhanxing Zhu. Interpreting adversarially trained convolutional neural networks. *arXiv preprint arXiv:1905.09797*, 2019.

Luisa M Zintgraf, Taco S Cohen, Tameem Adel, and Max Welling. Visualizing deep neural network decisions: Prediction difference analysis. *arXiv preprint arXiv:1702.04595*, 2017.

S1 SUPPLEMENT

S1.1 ADDITIONAL DETAILS ABOUT SST TASK

In Section 4.3 we show results of our method on biased variants of the SST dataset. Here we show examples of the biased sentences (for task 2 and 3 we only show sentences where the bias was present) in Figs. S1 to S3. For the first task, we insert two randomly chosen words in 100% of the sentences in the positive and negative class respectively. We chose two words (”text” for the positive class and ”video” for the negative class) that were not otherwise present in the data set but had a representation in Word2Vec.

For the second task, we chose to replace two common words (”the” and ”a”) in sentences where they appeared (27% of the dataset). We replaced the words such that one word would only appear in the positive and one word would only appear in the negative class. By choosing words that are semantically almost replaceable, we ensured that the normal sentence structure would not be broken such as with the first task.

For the third task we repeated the same procedure with two words (”he” and ”she”) that appeared in only 2% of the dataset. We did this to show that our method also works if the bias to be fixed appears only in a small section of the data set.

Positive

part of the charm of satin rouge is that it avoids the obvious with **text** humour and lightness .
text a screenplay more ingeniously constructed than ‘memento’
good fun **text**, good action, good acting, good dialogue, good pace, good cinematography .
dramas like **text** this make it human .

Negative

... begins with promise, but runs aground after being **video** snared in its own tangled plot .
the **video** movie is well done, but slow .
this orange has some juice , but it 's **video** far from fresh-squeezed .
as it is, **video** it 's too long and unfocused .

Figure S1: Example sentences from the variant 1 of the biased SST dataset with decoy variables in each sentence.

Positive

comes off as **a** touching , transcendent love story .
is most remarkable not because of its epic scope , but because of **a** startling intimacy
couldn't be better as **a** cruel but weirdly likable wasp matron
uses humor and **a** heartfelt conviction to tell that story about discovering your destination in life

Negative

to creep **the** living hell out of you
holds its goodwill close , but is relatively slow to come to **the** point
it 's not **the** great monster movie .
consider **the** dvd rental instead

Figure S2: Example sentences from the variant 2 of the SST dataset with artificially induced bias on articles (”the”, ”a”). Bias was only induced on the sentences where those articles were used (27% of the dataset).

Positive

pacino is the best **she**'s been in years and keener is marvelous

she showcases davies as a young woman of great charm , generosity and diplomacy

shows **she** 's back in form , with an astoundingly rich film .

proves once again that **she**'s the best brush in the business

Negative

green ruins every single scene **he**'s in, and the film, while it 's not completely wreaked, is seriously compromised by that

i'm sorry to say that this should seal the deal - arnold is not, nor will **he** be, back .

this is sandler running on empty , repeating what **he** 's already done way too often .

so howard appears to have had free rein to be as pretentious as **he** wanted

Figure S3: Example sentences from the variant 3 of the SST dataset with artificially induced bias on articles (”he”, ”she”). Bias was only induced on the sentences where those articles were used (2% of the dataset).

S1.2 Network architectures and training

S1.2.1 Network architectures

For the ISIC skin cancer task we used a pretrained VGG16 network retrieved from the PyTorch model zoo. We chose SGD as the optimizer with a learning rate of 0.01 and momentum of 0.9. Preliminary experiments with Adam as the optimizer showed worse results.

For both MNIST tasks, we use a standard convolutional network as retrieved with two convolutional channels followed by max pooling respectively and two fully connected layers:

Conv(20,5,5) - MaxPool() - Conv(50,5,5) - MaxPool - FC(256) - FC(10). The models were trained with Adam, using a weight decay of 0.001.

Penalizing explanations adds an additional hyperparameter, λ to the training. λ can either be set in proportion to the normal training loss or at a fixed rate. In this paper we did the latter. We expect that exploring the former could lead to a more stable training process. For all tasks λ was tested across a wide range between $[10^{-1}, 10^{4}]$.

The LSTM for the SST experiments consisted of two LSTM layers with 128 hidden units followed by a fully connected layer.

S1.2.2 ColorMNIST

For fixing the bias in the ColorMNIST task, we sample pixels from the distribution of non-zero pixels over the whole training set. This distribution is shown in Fig. S4

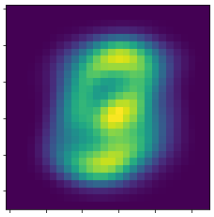

Figure S4: Sampling distribution for ColorMNIST

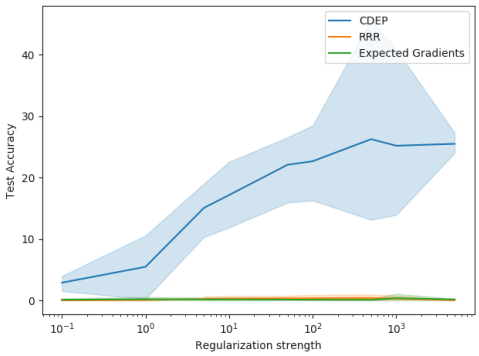

Figure S5: Results on ColorMNIST (Test Accuracy). All averaged over six runs. CDEP is the only method that captures and removes color bias.

S1.3 Runtime and memory requirements of different algorithms

We compared the runtime and memory requirements of the available regularization schemes when implemented in Pytorch. EGradients runs substantially slower since it requires resampling (the authors recommended 200 samples per example) with repeated forward and backward passes.

Memory usage and runtime were tested on the DecoyMNIST task with a batch size of 64. It is expected that the exact ratios will change depending on the complexity of the used network and batch size (since constant memory usage becomes disproportionally smaller with increasing batch size).

The memory usage was read by recording the memory allocated by PyTorch. Since Expected Gradients and RRR require two forward and backward passes, we only record the maximum memory usage. We ran experiments on a single Titan X.

Table S1: Runtime and memory usage of different schemes. Normalized that no regularization is 1

	Vanilla	CDEP	RRR	EGradients
Runtime	1.0	3.6	2.35	173.0
GPU memory usage	1.0	2.49	1.7	115.3

S1.4 IMAGE SEGMENTATION FOR ISIC SKIN CANCER

To obtain the binary maps of the patches for the skin cancer task, we first segmented the images using SLIC Achanta et al. (2012). Since the patches look quite distinct from the rest of the image, the patches were usually their own segment.

Subsequently we took the mean RGB and HSV values for all segments and filtered for segments which mean was far removed from the typical caucasian skin tone. Since different images were different from the typical skin color in different attributes, we filtered for those images recursively. As an example, in the image shown in Fig. S6, the patch has a much higher saturation than the rest of the image. For each image we exported a map as seen in Fig. S6.

Figure S6: Sample segmentation for the ISIC task.

S1.5 ADDITIONAL HEATMAP EXAMPLES FOR ISIC

We show additional examples from the test set of the skin cancer task in Figs. S7 and S8. We see that the importance maps for the unregularized and regularized network are very similar for cancerous images and non-cancerous images without patch. The patches are ignored by the network regularized with CDEP.

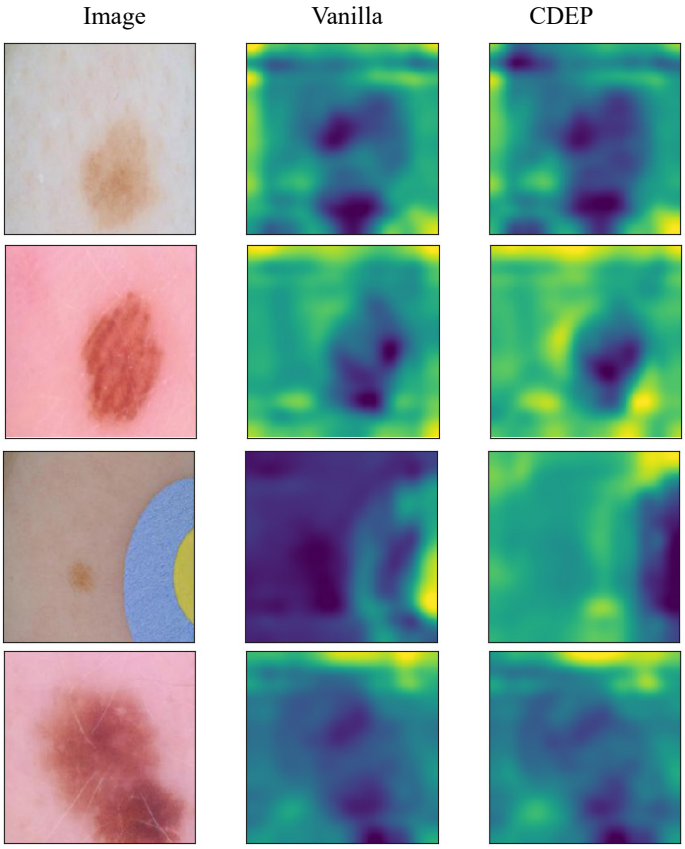

Figure S7: Heatmaps for benign samples from ISIC

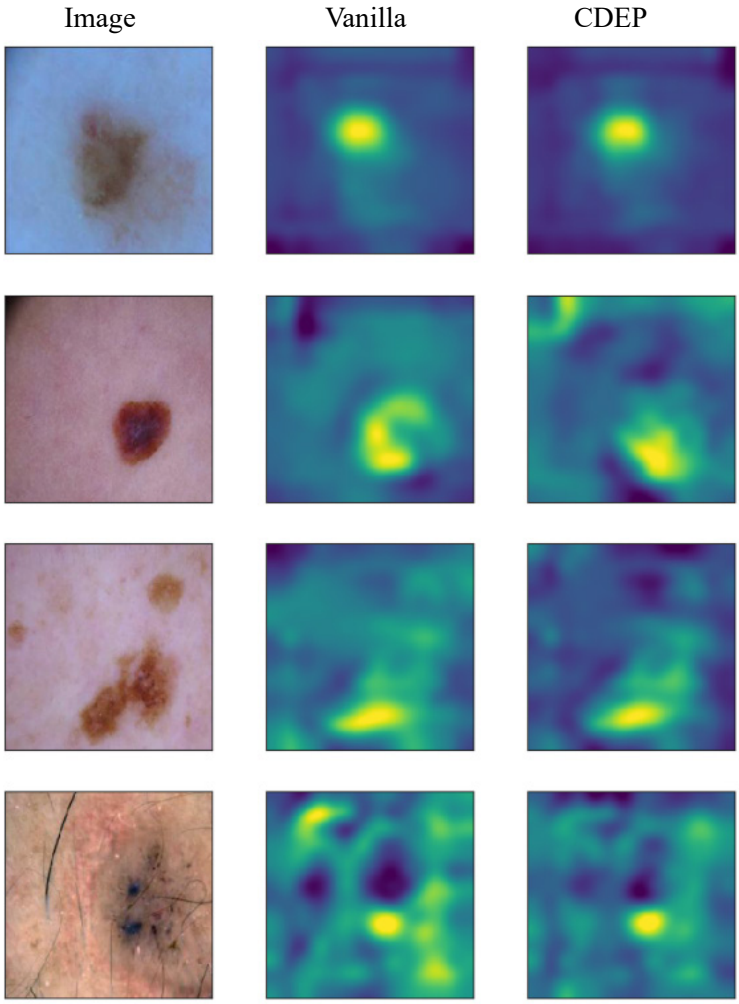

Figure S8: Heatmaps for cancerous samples from ISIC

A different spurious correlation that we noticed was that proportionally more images showing skin cancer will have a ruler next to the lesion. This is the case because doctors often want to show a reference for size if they diagnosed that the lesion is cancerous. Even though the spurious correlation is less pronounced (in a very rough cursory count, 13% of the cancerous and 5% of the benign images contain some sort of measure), the networks learnt to recognize and exploit this spurious correlation. This further highlights the need for CDEP, especially in medical settings.

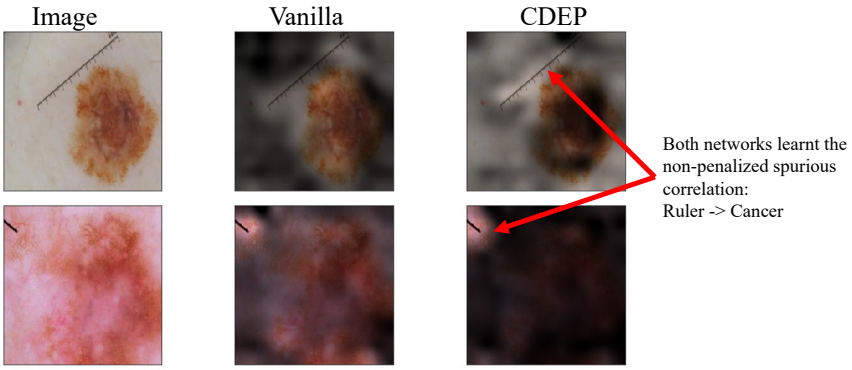

Figure S9: Both networks learnt that proportionally more images with malignant lesions feature a ruler next to the lesion. To make comparison easier, we visualize the heatmap by multiplying it with the image. Visible regions are important for classification.